International Journal of Science and Research (IJSR)
ISSN: 2319-7064
SJIF (2020): 7.803

A Short Review on Recent Advances in Coagulation Sensors for COVID-19 Disease Management

Navin Pai[1], Atul Sharma[2], Rupesh Kumar Mishra[3]

[1]Navin Pai, Former PDF-UCSD, Mumbai 400092-India

[2]Department of Pharmaceutical Chemistry, SGT College of Pharmacy, SGT University, Gurugram, Haryana 122505, India

[3]School of Materials Science and Engineering, Purdue University, West Lafayette, IN 47907-2045, USA

[1]Corresponding author Email: *n23pai[at]gmail.com*

Abstract: ***The COVID-19 disease caused by severe acute respiratory syndrome by the coronavirus-2 (SARS-CoV-2) has affected multiple world regions. COVID-19-induced coagulopathy (CIC) is characterized by a significant increase in D-dimer and fibrin split products and increases in activated partial thromboplastin and prothrombin time seen upon presentation. Biosensors are analytical tools that can provide fast, accurate, and reliable platforms for detecting viruses. This present review emphasizes an overview of the latest progress in biosensor-based diagnosis biomarkers of CIC.***

Keywords: Biosensors, SARS-CoV-2, COVID-19, Point of care device

1. Introduction

The COVID-19 pandemic has strained national health systems, leading to a health catastrophe[1] and an extraordinary socio-economic burden. Many countries, including India, relied on the detection of symptoms to identify and segregate patients affected by COVID-19, such as thermal screening and reports of fever and cough. [2]Real-time polymerase chain reaction (RT-PCR) on the virus nucleic acid employed as the golden standard testing approach. [3] However, these devices are centralized, requiring highly trained personnel and regular maintenance from skilled technicians. This adds to the operating cost and becomes inaccessible to most patients and clinicians worldwide. The World Health Organization (WHO) has called for research to create clinical diagnostic tools that increase accessibility in resource-limited settings with limited access to a central laboratory.

Managing and observing patients affected with COVID-19 in the emergency ward who may progress to intensive care requires constant monitoring of vital parameters and biomarkers specific to the conditions. The standard tests employed for detection and quantification like ELISA and spectrophotometry need medical personnel to collect blood and send to the specialised lab, with long turnaround times of approximately 2-4 hours. As a result, quick measurements are not available to clinicians who need real-time assessment of rapidly deteriorating conditions of severe COVID patients. One study found that 17% of their patients developed acute respiratory distress syndrome (ARDS), with 65% progressing to death from multiple organ failure. [4]The focus of this paper would be on particular emphasis on sensors that would enable clinicians to monitor coagulation parameters and routine haematological parameters, enabling them to arrive at a real-time risk assessment of such critical patients.

Diagnostic testing point-of-care (POC), conducted in the clinic or offsite, can be a handy tool for clinicians without waiting for days or even hours for sample transport and laboratory processing. [5]POC diagnostics have attracted increasing attention in clinics, especially in resource-poor regions. They are affordable, sensitive, user-friendly, rapid and robust, equipment-free, and deliverable to end-user. [6, 7] The various detection methods employed for the development of POC diagnostics, including electrochemical biosensors, fluorescence biosensors, surface-enhanced Raman scattering (SERS)-based biosensors, colorimetric biosensors, chemiluminescence biosensors, surface plasmon resonance (SPR)-based biosensors, and magnetic biosensors. [8-11]

1.1 Clinical Features

Clinical features of patients with SARS-CoV-2 are classified as mild, severe or critical, and sometimes asymptomatic. The mild symptoms are dry cough, fever, sore throat, nasal congestion, and muscle pain. [12, 13] Severe COVID-19 and bacterial pneumonia have similar symptoms, with both causing severe hypoxia requiring ventilatory support. In both cases, the pathology picture is characterized by extensive inflammatory cell recruitment to the lungs, a potent acute-phase reaction, and raised levels of pro-inflammatory cytokines.

The main routine tests requested for COVID-19 patients include complete blood count (CBC), assays investigating coagulation and fibrinolysis pathways such as prothrombin time (PT), activated partial thromboplastin time (aPTT), and D-dimers). [14, 15] Thus, the identification and diagnosis of severe or critical patients are critical using efficient haematology and coagulation parameters for risk classifications and to predict prognosis is a priority.

Licensed Under Creative Commons Attribution CC BY

The haematological analysis is the most widely performed test in the clinic. In almost all admissions, clinicians want to assess with CBC results. The first haematological picture of SARS COVID-2 came from China. [4, 15] The study revealed that the total number of peripheral white blood cells is typical or the lymphocyte count reduced in patients at the early stage of COVID-19. *Tan et al* conducted a descriptive and predictive study. They found that lymph cell % (Lym%) was inversely related to the severity and prognosis of patients and could be used to predict the severity and prognosis of patients with COVID-19. Counts of eosinophils and platelets were significantly lower in patients with acute disease than those with severe disease. [16] Thrombocytopenia was observed in 14%and moderate (6%) conditions. [17]

Sensors for routine Haematological parameters:

Microfluidic devices for cell counting have been reported using coulter counters and AC signals. Holmes *et al*. have shown the total leukocyte count and its differential using multi-frequency impedance cytometry. [4, 18]. Most of the reported microfluidic counters were based on impedance cell counting technology. Nguyen *et al*. characterized a biochip for CBC using a small population subset. [19] Smith *et al*. have shown an image-based device for complete blood cell counts with off-chip sample preparation. [20]Rahul *et al.* developed a unique, low-cost device as a blood cell counting platform by exploiting the difference in cells densities for separation in transparent microfluidic channels and implemented a label-free imaging method to estimate the separated cells within the microfluidic disc. [21] The developed device is a simple spinning disc, which estimates the parameters such as hematocrit, hemoglobin, red blood cell (RBC), white blood cell (WBC), and platelet counts with an accuracy > 95% as compared to an automated haematology analyser.

1.2 Coagulation Parameters

In COVID-19 patients, abnormalities of mechanisms of primary haemostasis, coagulation and fibrinolytic parameters have been reported and related with severe illness with ARDS development.

Initial studies reporting the complete coagulation parameters of 183 consecutive patients with COVID-19 pneumonia revealed significantly higher levels of fibrin-related markers (D-dimer and FDP and longer PT at admission, while lower fibrinogen levels and antithrombin (AT) activity at the end of the hospitalization, in non-survivors as compared to survivors. [14]The non-survivors and survivor data matched the criteria for disseminated intravascular coagulation (DIC) in the later stages of pneumonia, according to the International Society on Thrombosis and Haemostasis (ISTH). This data has underlined the importance of coagulation markers monitoring in all COVID-19 cases, leading to ISTH release of guidelines for the management of coagulopathy in COVID-19. Coagulation dysfunction not only could reflect the severity of the disease but also vary according to the stage of the disease, suggesting a careful monitoring of these parameters during hospitalization.

Table 1: Difference in coagulation parameters between COVID-19 and conventional sepsis (Adopted from Hadid et al 2021, copyright Elsevier 2021) [22]

Variable	COVID-19 spesis	Conventional spesis
aPTT	N/ ↑	↑↑/↑↑↑
PT	N/ ↑	↑↑/↑↑↑
Fibrinogen	↑↑↑/ ↑↑/↓	↑↑↑/ ↑↑/↓
Thrombocytopenia	N/ ↓	↓↓/↓↓↓
FSP	↑/ ↑↑	↑↑/ ↑↑↑
D-Dimer	↑↑/ ↑↑↑	↑/ ↑↑
Schistocytes on peripheral blood smear	Not present	Frequent

D-dimers are one of several fragments that are produced when plasmin cleaves fibrin, thus, they represent the expression of fibrin formation and degradation occurring during the fibrinolytic activity of clot. [23]

D-dimer tests have a highly negative predictive value, allowing the exclusion of an ongoing process of clot formation and is used to exclude DVT in a patient with low pretext probability. [24]A highly sensitive D-dimer assay can exclude DVT in a moderate-risk patient, whereas a moderately sensitive D-dimer assay needs additional testing for the final diagnosis. [25]A broad activation of the coagulation system, as demonstrated by elevated a PPT and PT, as well as significantly elevated D-dimer values, with the latter notably enhanced and are associated with poor prognosis. [4, 16]Evidence of disseminated intravascular coagulation leads to increased mortality rateCOVID-19. [15] In severe COVID-19, the clinical picture shows a high incidence of pulmonary and peripheral venous thromboembolic (VTE) disease, stroke and acute coronary syndromes, even in patients receiving prophylactic heparin. [26-29]The development of microthrombi in lung capillaries could explain the profound hypoxia seen in some patients with COVID-19, and similar microthrombi may contribute to renal and cardiac involvement. [30-33]It becomes imperative to differentiate severe patients from non-severe patients to improve the cure rate of COVID-19.

1.3 Biosensors for detecting D-Dimer:

Enzyme-linked immunosorbent assays (ELISA) method is considered a gold standard test because of high sensitivity for low-levels of D-dimer. With a turnaround time of 2–4 hours and a moderate specificity, this is a time-consuming approach. Latex-enhanced immunoturbidimetric and whole-blood assays are the other procedures available for D-dimer measurement, with the latter having the advantage of being performed at the bedside, with a turnaround time of 2–5 minutes and a greater specificity, but the disadvantage of a lower sensitivity. [34]

Developing an electrochemical sensor, in the case of D-dimer, all literature is based on the use of a selective antibody. One of the first work came from Rowe *et al* developed a sandwich fluoroimmunoassay in the sensing region of an evanescent wave biosensor. [34]In 11 minutes, physiological amounts of D-dimer and high molecular weight XL-FDP in buffer and plasma samples could be evaluated on calibrated fibres. ELISA and the fibre optic method were used to analyse samples from septic patients; fibre optic assay concentrations were well correlated with those reported by ELISA (r = 0.918); intra-and inter-assay errors were equivalent to those from ELISAs.

Licensed Under Creative Commons Attribution CC BY

A few electrochemical sensors have been developed for detecting D-dimers. Ibupoto *et al*. detected D-dimer using an electrode with zinc oxide (ZnO) nanotubes containing electrodeposited silver nanoparticles, while the antibody-antigen interaction on the surface of theworking electrode was measured potentiometrically. [35] Synthetic isopeptides formed on BSA were quantitatively analysed by a surface plasmon resonance-based biosensor method. The IgM antibody 81D4 was covalently attached to a carboxymethylated dextran surface, a CM5 surface, which reacted with the synthetic isopeptide as well as the natural isopeptide cross-link in D-dimer (but not with the non-cross-linked fibrin monomer). The interaction between the monoclonal 81D4 and the synthetic isopeptide was calculated to have a $4x10^{(-7)}$ M affinity. Good reactivity was also observed when human plasma spiked with this isopeptide was used as test solution.

Zhang *et al* established a photocatalysis-induced renewable graphene-FET (G-FET) biosensor for D-Dimer detection, using reduced graphene oxide (RGO) and RGO-encapsulated TiO2 composites to form a sandwiching RGO[at]TiO2 structure on a prefabricated FET sensor surface. [36] The sensitive detection of D-Dimer was achieved with the detection limits of 10 pg/mL in PBS and 100 pg/mL in serum, respectively. A few impedimetric approaches have also been published in recent years, and some important advantages are that the biomolecule orantibody-antigen binding could be directly detected without the use ofany mediators.

Chebil *et al* designed an immunosensor based on a single-chain antibody (ScAb) immobilized on a transducer surface and with a densely packed receptor layer, with the redox activity of a N-alpha bis (carboxymethyl)-L-lysine (ANTA) /Cu2+ complex attached to a polypyrrole backbone as the detector. [37]The resulting hybrid material: polypyrrole ANTA/metal complex/His-tag ScAb was characterized by AFM, surface plasmon resonance (SPR) and differential pulse voltammetry (DPV) for the optimization of the biosensor formation. The biosensor showed a remarkable variation in redox activity of the ANTA/Cu2+ complex after the D-dimer association with a binding constant Kd of 1 ng mL^{-1}. Electrochemical impedance spectroscopy (EIS) allowed monitoring D-dimer association with a linear response between 0.1 ng mL^{-1} and 500 ng mL^{-1} and a detection limit of 100 pg mL^{-1}in PBS is obtained. The biolayer also exhibited same sensitivity for the detection of d-dimer in human patient plasma samples. Bourigua *et al* developed impedimetric immunosensor based on functionalized carbon nanotubes (SWCNT-COOH) where the antibody (anti-D-dimer) was immobilized by covalent binding. The electrical properties and the morphology of the biolayer were characterized by electrochemical impedance spectroscopy (EIS), cyclic voltammetry and atomic force spectroscopy (AFM). [38] They obtained a sensitivity of 40.1 kΩ μM (-1) with a detection limit of 0.1 pg/mL (0.53 fM) and linear range from 0.1 pg/mL to 2 μg/mL (0.53 fM to 0.01 μM).

Marques *et al* developed a label-free approach with an electroactive SAM (2 thiols each with antibody and ferrocene and mounted on a commercial gold electrode. [39]The electronic transfer of this ferrocene varied according to the amount of D-dimer that had connected with the antibody.

A real-time dual-analyte assay based on a white light interference spectroscopy sensing platform for the simultaneous measurement of C-reactive protein (CRP) and D-dimer in human blood plasma was created by scanning the sensing surface. [40] The assay format involved direct detection of CRP whereas for D-dimer a two-site immunoassay employing a biotinylated reporter antibody and reaction with streptavidin was selected. The detection limits of 25ng/mL were obtained for both analytes (intra-and inter-assay CV values ranging from 3.6% to 7.7%, and from 4.8% to 9.5%, respectively).

Using a glassy carbon electrode and a series of ring permanent magnets, a homogeneous electrogenerated chemiluminescence (ECL) immunoassay for very sensitive measurement of individual biomarkers based on immunomagnetic beads and homogenous detection on a magnetic electrode was developed. [41]The model analyte was D-dimer antigen, while the magnetic capture probe was biotinylated D-dimer antibody linked to streptavidin-coated magnetic beads, and the ECL probe was ruthenium complex-labelled D-dimer antibody. The low detection limit of 1 ng/mL in magnetic enrich time of 2 min and the good magnetic regeneration for the detection of D-dimer were achieved.

Lakey *et al* developed a low-cost microfluidic device with a conveniently biofunctionalized interdigitated electrode (IDE) array and a portable impedimetric reader as a point-of-care (POC) device for the detection of D-dimer. [42]The IDE array elements, fabricated on a polyethylenenaphtalate (PEN) substrate, were biofunctionalized in situ after assembly of the microfluidic device by electro polymerisation of a copolymer of polypyrrole immobilised on a histidine tag anti-D-Dimer antibody. Measurement of clinical plasma sample with a D-dimer at concentration of 437 ng/mL with 15 biofunctionalized IDE array electrodes gave a ratio metric percentage of sample reading against the blank with an average value of 124 ± 15 at 95% confidence. Nadezdha *et al* created a multiplexed immunochromatographic assay using a traditional nitrocellulose membrane and microspot printing to create adjacent microfluidic "tracks" for multiplexed detection. [43]The 1 mm distance between tracks allowed for the detection of up to four different analytes. The lateral flow begins when the test strip is immersed in the sample, and reagents of various specificities move along their tracks without track degradation or reagent mixing (1-1.5 min compared with 10 min for common test strips). This assay format was used to detect cardiac and inflammatory markers (myoglobin, D-dimer, and C-reactive protein) in human blood, and it was found to have great repeatability (8 percent-15 percent coefficient of variation) when compared to traditional test working ranges.

Licensed Under Creative Commons Attribution CC BY

1.4 Potentials biomarkers with sensors development:

A- Fibrinogen:

QCM biosensor was developed by Yao *et al* to determine the activated partial thromboplastin time (APTT) for 120 anticoagulated plasma specimens. [44]A double-logarithmic plot of APTT vs fibrinogen concentration in the range of 1.58–6.30 g/L revealed a decent linear relationship. The QCM biosensor detects factor VIII in the range of 0.0185–0.111 mg/L. The results of the QCM biosensor were equivalent to those of commercial optical coagulometry, and an excellent agreement (correlation coefficient of 0.949 for fibrinogen and 0.948 for factor VIII) was achieved and accomplished in less than 10 minutes. Chen *et al* developed piezoelectric agglutination sensor to detect the fibrinogen agglutination reaction in patients with coronary heart diseases. [45]The results revealed a close relationship between the STAGO paramagnetic particle approach and the piezoelectric agglutination sensor method for Fibrinogen detection.0.91 (= 0.91) was the correlation coefficient was completed within 10 minutes.

Regmi *et al* developed an assay to detect plasmatic fibrinogen using electrical double layer gated AlGaN/GaN high electron mobility transistor biosensors without complex sample pre-treatment methods used in the traditional assays. [46]The sensor exhibited an ultra-low detection limit of 0.5 g/l and a detection range of 0.5–4.5 g/l in 1× PBS with 1% BSA. For very sensitive detection of fibrinogen, Jo S *et al* developed an erythrocyte membrane (EM)-blanketed biosensor conceptualized on localized surface plasmon resonance (LSPR). [47]By enhancing the LSPR signal, they demonstrated that fibrinogen detection was possible over a wide concentration range, 0.001–5.000 mg/mL, which can cover normal and pathological blood fibrinogen levels.

Bialkower *et al* demonstrate a handheld fibrinogen diagnostic that works with whole blood. [48]They premixed droplet of a whole blood sample and thrombin solution on a solid surface allowing it to clot, and later dropping a paper strip on top. The mobility of the blood down the strip, indicated the fibrinogen concentration. The diagnostic could easily measure plasma fibrinogen concentrations below 1.6 g/L for blood samples with haematocrit between 40 and 50%. The diluting blood samples increased the test's sensitivity and eliminated the effect of haematocrit and thrombin inhibitors. The test could be completed in 3–4 min, making it suitable for diagnosing early hypofibrinogenemia and allowing for fibrinogen replacement therapy in critically bleeding patients. Katz *et al* developed novel plasma fibrinogen point-of-care device when testing fibrinogen levels as low as 2 g/L. [49]

Aizawa *et al* developed a rapid immunosensor for fibrinogen and fibrin degradation products (FDP) that combines a quartz crystal microbalance (QCM) with the agglutination reaction of anti-FDP antibody immunized latex beads. [50]The results were obtained within 10min with a smart QCM-sensor. The detection range of the smart QCM-sensor is covered with screening concentration of FDP in serum (less than 10μgml−1 of FDP).

B-Thrombin:

Gosai *et al* reported a label-free sensitive detection of human α-thrombin by an aptamer-functionalized nano porous alumina membrane using a four-electrode electrochemical cell. [51]The sensor response to-thrombin was evaluated in the presence of a high concentration (500 M) of interfering protein, human serum albumin (HSA). The sensor's sensitivity was also tested against-thrombin, a modified version of-thrombin that lacks the aptamer binding epitope. In the presence of 500 mM HSA, the detection limit was 10 pM of-thrombin within an acceptable signal/noise ratio.

Liu *et al* reported a lateral flow aptasensor (LFA) for the simultaneous detection of platelet-derived growth factor-BB (PDGF-BB) and thrombin in spiked human serum samples. [52]

Two specific pairs of aptamers against PDGF-BB and thrombin, respectively, were used to prepare the LFA. Thiolated aptamers were immobilized on gold nanoparticle (AuNP) surface and biotinylated aptamers were immobilized on the test zones of an LFA nitrocellulose membrane. The assay involved the capture of PDGF-BB and thrombin simultaneously in sandwich-type formats between the capture aptamers on the test zones of LFA and AuNP-labelled detection aptamers. By combining the highly specific molecular recognition properties of aptamers with the unique properties of lateral flow assay, the optimized aptasensor was capable of simultaneously detecting 1.0 nM of PDGF-BB and 1.5 nM of thrombin in association with a 10-min assay time.

A label-free and highly sensitive impedimetric aptasensor was developed based on electropolymerized film. [53] The electro generation of a poly (pyrrole-nitrilotriacetic acid) (poly (pyrrole-NTA)) film onto the surface of electrodes followed by complexation of Cu^{2+} ions. The histidine labelled thrombin aptamer was immobilized onto the electrode through coordination of the histidine groups on the NTA–Cu^{2+} complex. A linear quantification of thrombin was obtained in the range 4.7×10^{-12}–5.0×10^{-10} mol L^{-1} with a sensitivity of 2838 Ω/log unit (R^2=0.9984).

Laura *et al* developed nanoporous anodic alumina (NAA) chemically modified with streptavidin as a platform for aptamer immobilization. [54]The immobilization of biotinylated thrombin binding aptamer (TBA) was monitored in real time by means of reflective interferometric spectroscopy (RIfS). The study could characterize in real time the path to immobilize TBA on the inner pore walls of NAA. This study provided an accurate label-free method to detect thrombin in real-time with high affinity and specificity.

Cho *et al* developed anaptamer-based surface enhanced resonance Raman scattering (SERRS) sensor. [55]The sensor achieved high sensitivity and a limit of detection of 100 pM by monitoring the SERRS signal change upon the single-step of thrombin binding to immobilized thrombin binding aptamer.

Coelho *et al* created an aptamer-based sensor based on two optical fibre configurations: long period gratings coated with

Licensed Under Creative Commons Attribution CC BY

a thin coating of titanium dioxide and surface plasmon resonance devices in optical fibres coated with a multilayer of gold and titanium dioxide. [56]The plasmonic device's sensitivity to the surrounding refractive index (RI) was higher than 3100 nm RIU1 in the RI range 1.335 to 1.355, a factor of 20 higher than the coated grating's sensitivity. With a wavelength shift of 3.5 nm and a resolution of 0.54 nM, 10 nM of thrombin could be detected.

Lin *et al* designed and conjugated thrombin-sensitive peptide substrates to the surface of nanoparticles to detect thrombi in living animals. [57]Following intravenous infusion, these "synthetic biomarkers" surveyed the host vasculature for coagulation and, in response to substrate cleavage by thrombin, released ligand-encoded reporters into the host urine. They further developed a companion 96-well immunoassay that utilized antibodies to bind specifically to the ligands, using mouse models of pulmonary embolism, the utility of urinary biomarker in differentiating between healthy and thrombotic states and correlation with the aggregate burden of clots formed in the lungs were obtained.

Matsuka *et al* devised a sensor for detecting an ethanol-free autologous thrombin in serum. [58]The ethanol-free autologous serum (AS) was prepared using the Thrombinator™ System (Arthrex, Inc., Naples, FL). Approximately 120 devices were tested with the blood of 30 healthy donors to determine the reliability and flexibility of the procedure. AS was prepared from both whole blood (WB) and platelet-poor plasma (PPP). Study endpoints were thrombin activity determined using a coagulation analyser and formation of cohesive bone graft composites objectively measured using a durometer. The average thrombin activity produced by this system from 24 donors was 20.6 ± 2.7 IU/mL for 13.4 ± 3.8 IU/mL for PPP which correlated to clot times of 3.9 and 5.9 seconds, respectively.

Nielsen *et al* developed the preparation of a key PTB risk biomarker, thrombin-antithrombin (TAT) [59]and characterized it using dot blots, MS, and microchip electrophoresis (μCE). The pH for fluorescently labelling TAT was also optimized using spectrofluorometer and spectrophotometry. The LOD of TAT was measured in μCE. Lastly, TAT was combined with six other PTB risk biomarkers and separated in μCE.

Dudani *et al* demonstrated the utility of a thrombin sensor to identify thrombosis and an MMP sensor to measure inflammation by formulating a subcutaneously administered sustained release system by using small PEG scaffolds (<10 nm) to promote diffusion into the bloodstream in a day. [60]This culminated in a development of a companion paper ELISA using printed wax barriers with nanomolar sensitivity for urinary reporters for point-of-care detection.

Cennamo *et al* developed a quick and low-cost biosensor using a plasmonic D-shaped plastic optical fibre (POF) sensor derivatized with an aptamer specialized for thrombin identification. [61]They created a functional interface using a self-assembled monolayer (SAM) made up of short Poly Ethylene Glycol (PEG) chains and biotin-modified PEG thiol in a ratio of 8: 2 mol: mol, with the latter serving as baits for aptamer binding via streptavidin chemistry (Figure 1). The optimized SAM composition allowed 112 ng/cm2 of aptamer to be immobilized. The detection of thrombin with the POF-Aptasensor took about 5–10 minutes, the attained Limit of Detection (LOD) was around 1 nM, and the detection range was 1.6–60 nM.

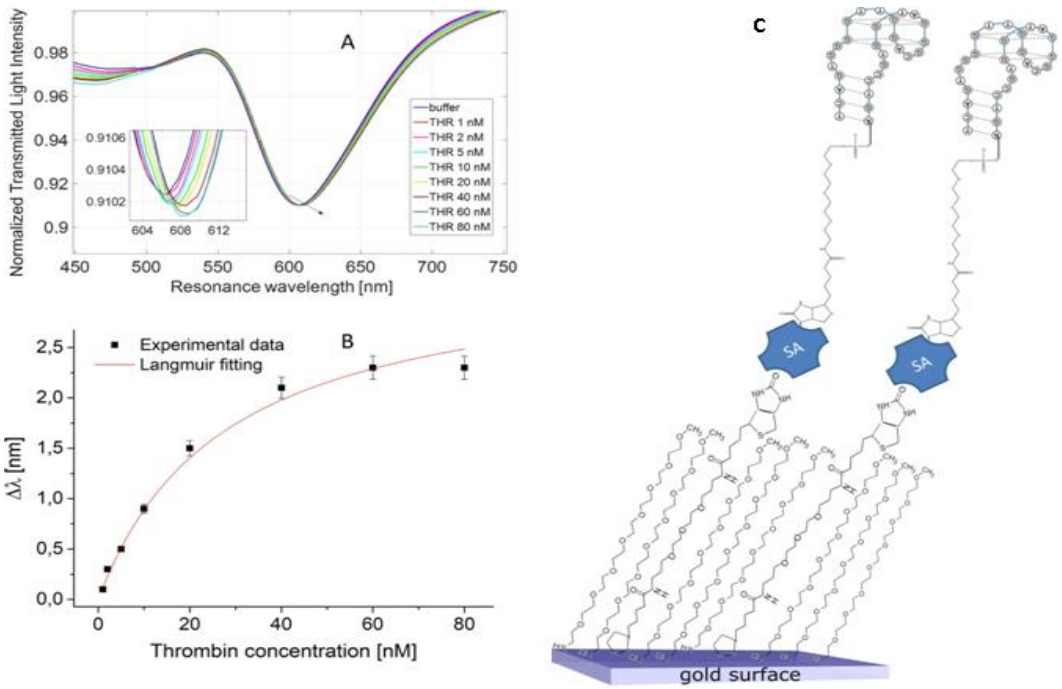

Figure 1: (A) SPR transmission spectra, normalized to the spectrum in air, for different concentrations of thrombin (1–80 nM). Inset: zoom of the resonance wavelengths region. (**B**) Plasmon resonance wavelength variation (Δλ), with respect to the blank, versus the concentration of THR (nM), with the Langmuir fitting to the experimental values and the error bars. Each experimental value is the average of 3 measurements obtained with three similar SPR-aptasensors (three similar SPR-POF platforms functionalized with the same bio-receptor); standard deviation (error bars) was within 5%. (**C)** Scheme of the functionalization process. A biotin functionalized reagent is inserted in the SAM composition; streptavidin layer is

Licensed Under Creative Commons Attribution CC BY

immobilized on it and finally a biotin modified DNA-aptamer is attached (adopted with permission from Cennamo et al 2019). [61]

C-PROTHROMBIN TIME (PT):

Williams *et al* developed a handheld point-of-care test (POCT) to measure PT using electrical transduction Low-cost PT sensors were fully printed using an aerosol jet printer and conductive inks of Ag nanoparticles, Ag nanowires, and carbon nanotubes. [62]The optimized operating frequency of this sensor was 15 kHz. When printed on polyimide, the PT sensor exhibited no variation in the measured clotting time, even when flexed to a 35 mm bend radius and showed 70% lower noise compared to measurement with a commercial potentiostat.

Tripathi *et al* created a portable, battery-operated optical sensor that measured changes in the viscoelastic characteristics of a drop of whole blood upon thromboplastin activation. [63]The optical sensor was used to measure PT/INR in 60 individuals, and the results were compared to the matching CCT values, revealing a strong correlation and good concordance between the two methods.

Based on parylene-C coated quartz crystal microbalance (QCM) dissipation monitoring and analysis, a unique smartphone-based blood coagulation diagnostic platform was developed. For fibrin trapping, the parylene-C coating created a strong and sticky surface. [64]The dissipation factor was calculated by evaluating the sensor's frequency response. All measured data was delivered via Bluetooth to a smartphone for calculation of dissipation and blood coagulation outcomes. This platform was used to measure two important coagulation indexes, aPTT and PT, and the adjusted R-square (R2) values for APTT and PT measures were 0.985 and 0.961, respectively, with commercial coagulation test platforms. A shear mode bulk acoustic resonator based on an inclined *c*-axis aluminum nitride (AlN) film for monitoring the prothrombin time (PT) along with its derived measure of international normalized ratio (INR), was developed. [65]Due to the viscosity change during the creation of fibers in blood, the device's resonant frequency reduced along with a step-ladder profile, displaying the sequential coagulation stages.

2. Conclusion

This review provides the recent advances and current opportunities for sensortechnologies of biomarkers related to COVID-19 and its comorbidities. Opportunities are present for targeting cytokines (ILs, TNFs, IFNs) and other biomarkers (CRPand glutamate). Government agencies should start actively funding for research into biosensing technologies. Biosensing technologies should be available in the same manner as glucometer technologies, which are affordable for many consumers. The detection of suchbiomolecules involved in many diseases and continued work would improve health outcomes. Unlike conventional techniques, biosensor technologies have the superior detection capability to provide an ultra-trace level of an analyte. Future biosensors research should be directed towards detecting SARS-CoV-2 in the aerosol, sewage discharge, and air droplets to detect viral spread in communities. It is imperative for middle income countries without ecosystem of rich countries to promote investments in biosensor research and development to facilitate the development of high-quality analytical devices that provide detection at the point of need.

References

[1] The Novel Coronavirus Pneumonia Emergency Response Epidemiology, T. The Epidemiological Characteristics of an Outbreak of 2019 Novel Coronavirus Diseases (COVID-19)-China, 2020. *China CDC Wkly* **2020**, *2*, 113-122.

[2] Bhat, M. A.; Rahman, S.; Rather, I. A.; Banday, M. I.; Syed, S.; Koser, H.; Kamal, M. A.; Minakshi, R.; Jan, A. T. Coronavirus Disease-2019 (COVID-19) in 2020: A Perspective Study of a Global Pandemic. *Current Pharmaceutical Design* **2021**, *27*, 3435-3443, doi: 10.2174/1381612826666201118112912.

[3] Yang, Y.; Yang, M.; Shen, C.; Wang, F.; Yuan, J.; Li, J.; Zhang, M.; Wang, Z.; Xing, L.; Wei, J.; et al. Evaluating the accuracy of different respiratory specimens in the laboratory diagnosis and monitoring the viral shedding of 2019-nCoV infections. *medRxiv* **2020**, 2020.2002.2011.20021493, doi: 10.1101/2020.02.11.20021493.

[4] Wang, D.; Hu, B.; Hu, C.; Zhu, F.; Liu, X.; Zhang, J.; Wang, B.; Xiang, H.; Cheng, Z.; Xiong, Y.; et al. Clinical Characteristics of 138 Hospitalized Patients With 2019 Novel Coronavirus-Infected Pneumonia in Wuhan, China. *Jama* **2020**, *323*, 1061-1069, doi: 10.1001/jama.2020.1585.

[5] Vandenberg, O.; Martiny, D.; Rochas, O.; van Belkum, A.; Kozlakidis, Z. Considerations for diagnostic COVID-19 tests. *Nat Rev Microbiol* **2021**, *19*, 171-183, doi: 10.1038/s41579-020-00461-z.

[6] Sista, R.; Hua, Z.; Thwar, P.; Sudarsan, A.; Srinivasan, V.; Eckhardt, A.; Pollack, M.; Pamula, V. Development of a digital microfluidic platform for point of care testing. *Lab on a Chip* **2008**, *8*, 2091-2104, doi: 10.1039/B814922D.

[7] Tram, D. T.; Wang, H.; Sugiarto, S.; Li, T.; Ang, W. H.; Lee, C.; Pastorin, G. Advances in nanomaterials and their applications in point of care (POC) devices for the diagnosis of infectious diseases. *Biotechnol Adv* **2016**, *34*, 1275-1288, doi: 10.1016/j. biotechadv.2016.09.003.

[8] Pai, A.; Khachaturian, A.; Chapman, S.; Hu, A.; Wang, H.; Hajimiri, A. A handheld magnetic sensing platform for antigen and nucleic acid detection. *Analyst* **2014**, *139*, 1403-1411, doi: 10.1039/c3an01947k.

[9] Tepeli, Y.; Ülkü, A. Electrochemical biosensors for influenza virus a detection: The potential of adaptation of these devices to POC systems. *Sensors and Actuators B: Chemical* **2018**, *254*, 377-384, doi: https://doi.org/10.1016/j. snb.2017.07.126.

[10] Nicolini, A. M.; McCracken, K. E.; Yoon, J. Y. Future developments in biosensors for field-ready Zika virus diagnostics. *J Biol Eng* **2017**, *11*, 7, doi: 10.1186/s13036-016-0046-z.

Licensed Under Creative Commons Attribution CC BY

[11] Citartan, M.; Tang, T. H. Recent developments of aptasensors expedient for point-of-care (POC) diagnostics. *Talanta* **2019**, *199*, 556-566, doi: 10.1016/j. talanta.2019.02.066.
[12] Guan, W. J.; Ni, Z. Y.; Hu, Y.; Liang, W. H.; Ou, C. Q.; He, J. X.; Liu, L.; Shan, H.; Lei, C. L.; Hui, D. S. C.; et al. Clinical Characteristics of Coronavirus Disease 2019 in China. *N Engl J Med* **2020**, *382*, 1708-1720, doi: 10.1056/NEJMoa2002032.
[13] Sharma, A.; Tiwari, S.; Deb, M. K.; Marty, J. L. Severe acute respiratory syndrome coronavirus-2 (SARS-CoV-2): a global pandemic and treatment strategies. *International Journal of Antimicrobial Agents* **2020**, *56*, 106054, doi: https://doi.org/10.1016/j. ijantimicag.2020.106054.
[14] Tang, N.; Li, D.; Wang, X.; Sun, Z. Abnormal coagulation parameters are associated with poor prognosis in patients with novel coronavirus pneumonia. *J Thromb Haemost* **2020**, *18*, 844-847, doi: 10.1111/jth.14768.
[15] Huang, C.; Wang, Y.; Li, X.; Ren, L.; Zhao, J.; Hu, Y.; Zhang, L.; Fan, G.; Xu, J.; Gu, X.; et al. Clinical features of patients infected with 2019 novel coronavirus in Wuhan, China. *Lancet* **2020**, *395*, 497-506, doi: 10.1016/s0140-6736 (20) 30183-5.
[16] Yan, B.; Yang, J.; Xie, Y.; Tang, X. Relationship between blood eosinophil levels and COVID-19 mortality. *World Allergy Organ J* **2021**, *14*, 100521, doi: 10.1016/j. waojou.2021.100521.
[17] Bao, C.; Tao, X.; Cui, W.; Yi, B.; Pan, T.; Young, K. H.; Qian, W. SARS-CoV-2 induced thrombocytopenia as an important biomarker significantly correlated with abnormal coagulation function, increased intravascular blood clot risk and mortality in COVID-19 patients. *Exp Hematol Oncol* **2020**, *9*, 16, doi: 10.1186/s40164-020-00172-4.
[18] Holmes, D.; Pettigrew, D.; Reccius, C. H.; Gwyer, J. D.; van Berkel, C.; Holloway, J.; Davies, D. E.; Morgan, H. Leukocyte analysis and differentiation using high speed microfluidic single cell impedance cytometry. *Lab on a Chip* **2009**, *9*, 2881-2889, doi: 10.1039/B910053A.
[19] Nguyen, J.; Wei, Y.; Zheng, Y.; Wang, C.; Sun, Y. On-chip sample preparation for complete blood count from raw blood. *Lab on a Chip* **2015**, *15*, 1533-1544, doi: 10.1039/C4LC01251H.
[20] Smith, Z. J.; Gao, T.; Chu, K.; Lane, S. M.; Matthews, D. L.; Dwyre, D. M.; Hood, J.; Tatsukawa, K.; Heifetz, L.; Wachsmann-Hogiu, S. Single-step preparation and image-based counting of minute volumes of human blood. *Lab on a Chip* **2014**, *14*, 3029-3036, doi: 10.1039/C4LC00567H.
[21] Agarwal, R.; Sarkar, A.; Bhowmik, A.; Mukherjee, D.; Chakraborty, S. A portable spinning disc for complete blood count (CBC). *Biosens Bioelectron* **2020**, *150*, 111935, doi: 10.1016/j. bios.2019.111935.
[22] Hadid, T.; Kafri, Z.; Al-Katib, A. Coagulation and anticoagulation in COVID-19. *Blood Reviews* **2021**, *47*, 100761, doi: https://doi.org/10.1016/j. blre.2020.100761.
[23] Adam, S. S.; Key, N. S.; Greenberg, C. S. D-dimer antigen: current concepts and future prospects. *Blood* **2009**, *113*, 2878-2887, doi: 10.1182/blood-2008-06-165845.
[24] Lecourvoisier, C.; Toulon, P. [Value of D-dimer measurement in the exclusion diagnosis of pulmonary embolism]. *Ann Biol Clin (Paris)* **2001**, *59*, 693-700.
[25] Anderson, D. R.; Wells, P. S. D-dimer for the diagnosis of venous thromboembolism. *Curr Opin Hematol* **2000**, *7*, 296-301, doi: 10.1097/00062752-200009000-00007.
[26] Luo, W.; Yu, H.; Gou, J.; Li, X.; Sun, Y.; Li, J.; Liu, L. *Clinical Pathology of Critical Patient with Novel Coronavirus Pneumonia (COVID-19): Pulmonary Fibrosis and Vascular Changes including Microthrombosis Formation firstly Found*; 2020.
[27] Danzi, G. B.; Loffi, M.; Galeazzi, G.; Gherbesi, E. Acute pulmonary embolism and COVID-19 pneumonia: a random association? *Eur Heart J* **2020**, *41*, 1858, doi: 10.1093/eurheartj/ehaa254.
[28] Li, T.; Lu, H.; Zhang, W. Clinical observation and management of COVID-19 patients. *Emerg Microbes Infect* **2020**, *9*, 687-690, doi: 10.1080/22221751.2020.1741327.
[29] Wang, T.; Chen, R.; Liu, C.; Liang, W.; Guan, W.; Tang, R.; Tang, C.; Zhang, N.; Zhong, N.; Li, S. Attention should be paid to venous thromboembolism prophylaxis in the management of COVID-19. *Lancet Haematol* **2020**, *7*, e362-e363, doi: 10.1016/s2352-3026 (20) 30109-5.
[30] Lehman, C. M.; Wilson, L. W.; Rodgers, G. M. Analytic validation and clinical evaluation of the STA LIATEST immunoturbidimetric D-dimer assay for the diagnosis of disseminated intravascular coagulation. *Am J Clin Pathol* **2004**, *122*, 178-184, doi: 10.1309/x4yn-001g-u51n-gg9y.
[31] Xu, Z.; Shi, L.; Wang, Y.; Zhang, J.; Huang, L.; Zhang, C.; Liu, S.; Zhao, P.; Liu, H.; Zhu, L.; et al. Pathological findings of COVID-19 associated with acute respiratory distress syndrome. *Lancet Respir Med* **2020**, *8*, 420-422, doi: 10.1016/s2213-2600 (20) 30076-x.
[32] Hanley, B.; Lucas, S. B.; Youd, E.; Swift, B.; Osborn, M. Autopsy in suspected COVID-19 cases. *J Clin Pathol* **2020**, *73*, 239-242, doi: 10.1136/jclinpath-2020-206522.
[33] Barton, L. M.; Duval, E. J.; Stroberg, E.; Ghosh, S.; Mukhopadhyay, S. COVID-19 Autopsies, Oklahoma, USA. *Am J Clin Pathol* **2020**, *153*, 725-733, doi: 10.1093/ajcp/aqaa062.
[34] Rowe, C. A.; Bolitho, J. S.; Jane, A.; Bundesen, P. G.; Rylatt, D. B.; Eisenberg, P. R.; Ligler, F. S. Rapid detection of D-dimer using a fiber optic biosensor. *Thrombosis and haemostasis* **1998**, *59*, 94-98.
[35] Ibupoto, Z. H.; Jamal, N.; Khun, K.; Liu, X.; Willander, M. A potentiometric immunosensor based on silver nanoparticles decorated ZnO nanotubes, for the selective detection of d-dimer. *Sensors and Actuators B: Chemical* **2013**, *182*, 104-111, doi: https://doi.org/10.1016/j. snb.2013.02.084.
[36] Zhang, C.; Xu, J. Q.; Li, Y. T.; Huang, L.; Pang, D. W.; Ning, Y.; Huang, W. H.; Zhang, Z.; Zhang, G. J. Photocatalysis-Induced Renewable Field-Effect Transistor for Protein Detection. *Anal Chem* **2016**, *88*, 4048-4054, doi: 10.1021/acs. analchem.6b00374.

Licensed Under Creative Commons Attribution CC BY

[37] Chebil, S.; Hafaiedh, I.; Sauriat-Dorizon, H.; Jaffrezic-Renault, N.; Errachid, A.; Ali, Z.; Korri-Youssoufi, H. Electrochemical detection of D-dimer as deep vein thrombosis marker using single-chain D-dimer antibody immobilized on functionalized polypyrrole. *Biosens Bioelectron* **2010**, *26*, 736-742, doi: 10.1016/j. bios.2010.06.048.

[38] Bourigua, S.; Hnaien, M.; Bessueille, F.; Lagarde, F.; Dzyadevych, S.; Maaref, A.; Bausells, J.; Errachid, A.; Renault, N. J. Impedimetric immunosensor based on SWCNT-COOH modified gold microelectrodes for label-free detection of deep venous thrombosis biomarker. *Biosensors and Bioelectronics* **2010**, *26*, 1278-1282, doi: https://doi.org/10.1016/j. bios.2010.07.004.

[39] Marques, S. M.; Santos, A.; Gonçalves, L. M.; Sousa, J. C.; Bueno, P. R. Sensitive label-free electron chemical capacitive signal transduction for D-dimer electroanalysis. *Electrochimica Acta* **2015**, *182*, 946-952, doi: https://doi.org/10.1016/j. electacta.2015.09.169.

[40] Koukouvinos, G.; Petrou, P.; Misiakos, K.; Drygiannakis, D.; Raptis, I.; Stefanitsis, G.; Martini, S.; Nikita, D.; Goustouridis, D.; Moser, I.; et al. Simultaneous determination of CRP and D-dimer in human blood plasma samples with White Light Reflectance Spectroscopy. *Biosens Bioelectron* **2016**, *84*, 89-96, doi: 10.1016/j. bios.2015.11.094.

[41] Wei, Y.; Wang, Y.; Wang, J.; Yang, X.; Qi, H.; Gao, Q.; Zhang, C. Homogeneous electrogenerated chemiluminescence immunoassay for the detection of biomarkers by magnetic preconcentration on a magnetic electrode. *Analytical and Bioanalytical Chemistry* **2019**, *411*, 4203-4211, doi: 10.1007/s00216-019-01830-1.

[42] Lakey, A.; Ali, Z.; Scott, S. M.; Chebil, S.; Korri-Youssoufi, H.; Hunor, S.; Ohlander, A.; Kuphal, M.; Marti, J. S. Impedimetric array in polymer microfluidic cartridge for low cost point-of-care diagnostics. *Biosens Bioelectron* **2019**, *129*, 147-154, doi: 10.1016/j. bios.2018.12.054.

[43] Byzova, N. A.; Urusov, A. E.; Zherdev, A. V.; Dzantiev, B. B. Multiplex highly sensitive immunochromatographic assay based on the use of nonprocessed antisera. *Analytical and bioanalytical chemistry* **2018**, *410*, 1903-1910, doi: 10.1007/s00216-018-0853-9.

[44] Yao, C.; Qu, L.; Fu, W. Detection of Fibrinogen and Coagulation Factor VIII in Plasma by a Quartz Crystal Microbalance Biosensor. *Sensors* **2013**, *13*, 6946-6956.

[45] Chen, Q.; Hua, X.; Fu, W.; Liu, D.; Chen, M.; Cai, G. Quantitative Determination of Fibrinogen of Patients with Coronary Heart Diseases through Piezoelectric Agglutination Sensor. *Sensors* **2010**, *10*, 2107-2118.

[46] Regmi, A.; Sarangadharan, I.; Chen, Y.-W.; Hsu, C.-P.; Lee, G.-Y.; Chyi, J.-I.; Shiesh, S.-C.; Lee, G.-B.; Wang, Y.-L. Direct detection of fibrinogen in human plasma using electric-double-layer gated AlGaN/GaN high electron mobility transistors. *Applied Physics Letters* **2017**, *111*, 082106, doi: 10.1063/1.5000247.

[47] Jo, S.; Kim, I.; Lee, W.; Kim, M.; Park, J.; Lee, G.; Yoon, D. S.; Park, J. Highly sensitive and wide-range nanoplasmonic detection of fibrinogen using erythrocyte membrane-blanketed nanoparticles. *Biosens Bioelectron* **2019**, *135*, 216-223, doi: 10.1016/j. bios.2019.04.030.

[48] Bialkower, M.; Manderson, C. A.; McLiesh, H.; Tabor, R. F.; Garnier, G. Paper Diagnostic for Direct Measurement of Fibrinogen Concentration in Whole Blood. *ACS Sens* **2020**, *5*, 3627-3638, doi: 10.1021/acssensors.0c01937.

[49] Katz, R.; Efremov, V.; Mooney, C.; El-Khuffash, A.; Heaphy, L.; Cosgrave, D.; Loughrey, J.; Thornton, P. Assessment of the reliability and validity of a novel point-of-care fibrinogen (F-Point) device against an industry standard at fibrinogen levels >2 g/L in non-haemorrhage scenarios. *Int J Obstet Anesth* **2020**, *43*, 91-96, doi: 10.1016/j. ijoa.2020.04.001.

[50] Aizawa, H.; Kurosawa, S.; Tozuka, M.; Park, J.-W.; Kobayashi, K. Rapid detection of fibrinogen and fibrin degradation products using a smart QCM-sensor. *Sensors and Actuators B: Chemical* **2004**, *101*, 150-154, doi: https://doi.org/10.1016/j. snb.2004.02.057.

[51] Gosai, A.; Hau Yeah, B. S.; Nilsen-Hamilton, M.; Shrotriya, P. Label free thrombin detection in presence of high concentration of albumin using an aptamer-functionalized nanoporous membrane. *Biosensors and Bioelectronics* **2019**, *126*, 88-95, doi: https://doi.org/10.1016/j. bios.2018.10.010.

[52] Liu, G.; Gurung, A. S.; Qiu, W. Lateral Flow Aptasensor for Simultaneous Detection of Platelet-Derived Growth Factor-BB (PDGF-BB) and Thrombin. *Molecules* **2019**, *24*, 756.

[53] Xu, H.; Gorgy, K.; Gondran, C.; Le Goff, A.; Spinelli, N.; Lopez, C.; Defrancq, E.; Cosnier, S. Label-free impedimetric thrombin sensor based on poly (pyrrole-nitrilotriacetic acid)-aptamer film. *Biosensors and Bioelectronics* **2013**, *41*, 90-95, doi: https://doi.org/10.1016/j. bios.2012.07.044.

[54] Pol, L.; Acosta, L. K.; Ferré-Borrull, J.; Marsal, L. F. Aptamer-Based Nanoporous Anodic Alumina Interferometric Biosensor for Real-Time Thrombin Detection. *Sensors* **2019**, *19*, 4543.

[55] Cho, H.; Baker, B. R.; Wachsmann-Hogiu, S.; Pagba, C. V.; Laurence, T. A.; Lane, S. M.; Lee, L. P.; Tok, J. B. H. Aptamer-based SERRS sensor for thrombin detection. *Nano Lett* **2008**, *8*, 4386-4390, doi: 10.1021/nl802245w.

[56] Coelho, L.; Marques Martins de Almeida, J. M.; Santos, J. L.; da Silva Jorge, P. A.; Martins, M. C. L.; Viegas, D.; Queirós, R. B. Aptamer-based fiber sensor for thrombin detection. *J Biomed Opt* **2016**, *21*, 87005, doi: 10.1117/1. jbo.21.8.087005.

[57] Lin, K. Y.; Kwong, G. A.; Warren, A. D.; Wood, D. K.; Bhatia, S. N. Nanoparticles that sense thrombin activity as synthetic urinary biomarkers of thrombosis. *ACS Nano* **2013**, *7*, 9001-9009, doi: 10.1021/nn403550c.

[58] Matuska, A. M.; Klimovich, M. K.; Chapman, J. R. An Ethanol-Free Autologous Thrombin System. *J Extra Corpor Technol* **2018**, *50*, 237-243.

[59] Nielsen, J. B.; Nielsen, A. V.; Carson, R. H.; Lin, H. L.; Hanson, R. L.; Sonker, M.; Mortensen, D. N.; Price, J. C.; Woolley, A. T. Analysis of thrombin-antithrombin complex formation using microchip electrophoresis and mass spectrometry.

Licensed Under Creative Commons Attribution CC BY

Electrophoresis **2019**, *40*, 2853-2859, doi: 10.1002/elps.201900235.

[60] Dudani, J. S.; Buss, C. G.; Akana, R. T. K.; Kwong, G. A.; Bhatia, S. N. Sustained-Release Synthetic Biomarkers for Monitoring Thrombosis and Inflammation Using Point-of-Care Compatible Readouts. *Advanced Functional Materials* **2016**, *26*, 2919-2928, doi: https://doi.org/10.1002/adfm.201505142.

[61] Cennamo, N.; Pasquardini, L.; Arcadio, F.; Vanzetti, L. E.; Bossi, A. M.; Zeni, L. D-shaped plastic optical fibre aptasensor for fast thrombin detection in nanomolar range. *Scientific Reports* **2019**, *9*, 18740, doi: 10.1038/s41598-019-55248-x.

[62] Williams, N. X.; Carroll, B.; Noyce, S. G.; Hobbie, H. A.; Joh, D. Y.; Rogers, J. G.; Franklin, A. D. Fully printed prothrombin time sensor for point-of-care testing. *Biosens Bioelectron* **2021**, *172*, 112770, doi: 10.1016/j. bios.2020.112770.

[63] Tripathi, M. M.; Egawa, S.; Wirth, A. G.; Tshikudi, D. M.; Van Cott, E. M.; Nadkarni, S. K. Clinical evaluation of whole blood prothrombin time (PT) and international normalized ratio (INR) using a Laser Speckle Rheology sensor. *Scientific Reports* **2017**, *7*, 9169, doi: 10.1038/s41598-017-08693-5.

[64] Yao, J.; Feng, B.; Zhang, Z.; Li, C.; Zhang, W.; Guo, Z.; Zhao, H.; Zhou, L. Blood Coagulation Testing Smartphone Platform Using Quartz Crystal Microbalance Dissipation Method. *Sensors (Basel)* **2018**, *18*, doi: 10.3390/s18093073.

[65] Song, S.; Chen, D.; Wang, H.; Li, C.; Wang, W.; Yu, W.; Wang, Y.; Guo, Q. Shear Mode Bulk Acoustic Resonator Based on Inclined c-Axis AlN Film for Monitoring of Human Hemostatic Parameters. *Micromachines* **2018**, *9*, 501.

Licensed Under Creative Commons Attribution CC BY